Geologie en Mijnbouw **68**: 285–296, 1989.

A case study on the hydrocarbon geology of Upper Permian (Zechstein-3) carbonates in licence P6, the Netherlands' offshore.

A.B. van der Poel
Spoorlaan 42, 3721 PC Bilthoven, The Netherlands

Received 21 July 1988; accepted in revised form 25 January 1989

Key words: Upper Permian carbonates, Netherlands offshore, shallowing upwards sequence, diagenetic sequences, leaching, porosity, burial graph

Abstract

Permian (Zechstein-3) carbonates in the P6 block, the Netherlands' offshore, were deposited in a subtidal-intertidal-supratidal setting, in an overall shallowing-upwards mega sequence. Interpreted diagenetic events include in order of occurrence: lithification, dessication, early leaching, dolomitisation, anhydritisation, calcitisation and also late leaching, compaction/stylolitisation and late fracturation. The diagenetic sequence is related to the reconstructed burial history by plotting on a burial graph. Present diagenetic porosity (Moldic- intraparticle- vuggy- (enlarged) intercrystalline- fracture porosity) predates renewed hydrocarbon gas generation. Gas generation is continuing today.

Introduction

This study investigates the porosity development, diagenesis and hydrocarbon geology of Upper Permian (Zechstein-3) basin fringe carbonates in production licence P6. The Zechstein carbonates are locally gas-bearing in the P6 region. Production license P6 is located in the southern part of the Broad Fourteens Basin (Figs. 1 and 2). The Broad Fourteens Basin is a late Jurassic structural overprint on the older, Hercynian trends.

Offshore data are released from confidential files after ten years. Cores and core data from released wells P6-1, P6-2 and P6-3 were analysed. Exploration well P6-1 was drilled in 1968 and proved gas production from Zechstein-3 carbonates. Outstep well P6-2 did not find gas and was plugged back in 1969. Well P6-3, which was drilled on trend with P6-1, penetrated gas-bearing Zechstein-3 carbonates in 1976. Gas productive Triassic sandstones are also present in the licence, but they are not considered in the present paper.

Results of this study should improve the understanding of reservoir distribution within Zechstein-3 carbonates of the Netherlands offshore, which is of use to the oil and gas industry.

Geological setting

Stratigraphy

The stratigraphic subdivision of the Upper Permian in the Broad Fourteens area is shown in Fig. 3. Four cycles of carbonate/evaporite deposits are generally recognised (NAM & RGD, 1980).

In the basin fringe area of the southern Netherlands the Upper Permian is rich in siliciclastics. The clastics content decreases rapidly towards the north, where thick sequences of basinal halites are present. Van Adrichem Boogaert & Burgers

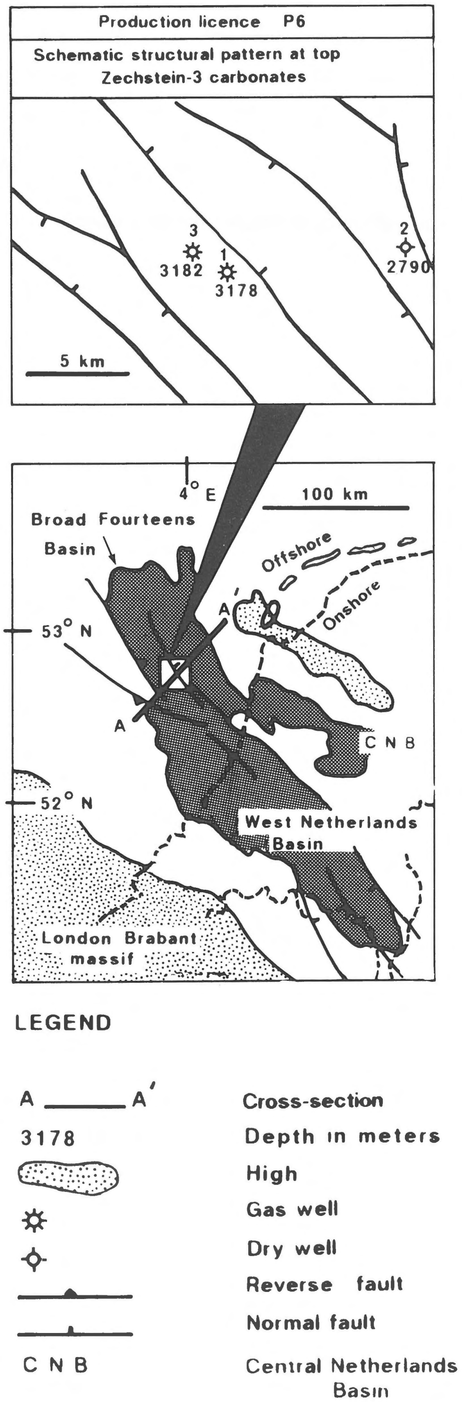

Fig. 1. Location map showing production licence P6. The position of geological cross section (A-A°), see Fig. 2, is indicated. The locations of gas wells P6-1, P6-3 and dry well P6-2 are shown in the inset.

(1983) described the general paleogeography, with a river system flowing from the London-Brabant Massif in the south, via a coastal area, into the basin.

The Zechstein-3 carbonates in a basin fringe development were investigated in the P6 area (Fig. 3). Isopachs of the Zechstein-3 carbonates have a clear N110° E trend (Fig. 4). The thickness ranges from zero to sixty metres. Towards the basin centre, the Zechstein-3 carbonates thin rapidly, grading into anhydrites and carbonates (Figs. 3, 4).

Tectonic history

The Upper Permian (Zechstein) was covered by an estimated 2000 metres of Triassic, Lower and Middle Jurassic sediments. During the late Jurassic, northwest – southeast trending fault zones developed (Oele et al. 1981; Ziegler, 1982) and the Broad Fourteens Basin, the West Netherlands Basin and the Central Netherlands Basin came into being (Fig. 1). Sedimentation was interrupted at the Oxfordian-Kimmeridgian boundary and the Upper Jurassic is developed in a paralic facies, (NAM & RGD, 1980) as is also evidenced by P6 well data. Differential subsidence continued in the basin with concurrent erosion of the highs in adjacent areas (Oele et al., 1981). During Late Cretaceous times the Permian carbonates subsided to some 4000 metres in the area. The area became inverted at the end of the Cretaceous and subsided again to deeper levels during the Cainozoic (Oele et al., 1981; Van Wijhe, 1987).

Previous work on Zechstein carbonates

Previous work on the stratigraphy, the sedimentology and the reservoir properties of the Permian carbonates in the Netherlands is reported by Brueren, (1959), Visser, (1963), Maureau & Van Wijhe, (1979), Clark, (1980a), NAM & RGD, (1980), Van Adrichem Boogaert & Burgers, (1983) and Van Lith, (1983). Clark (1980b, 1986) and Van der Poel (1987) studied diagenesis and porosity evolution.

No studies on the porosity development and diagenesis of the Permian Zechstein-3 in production licence P6 have been published previously.

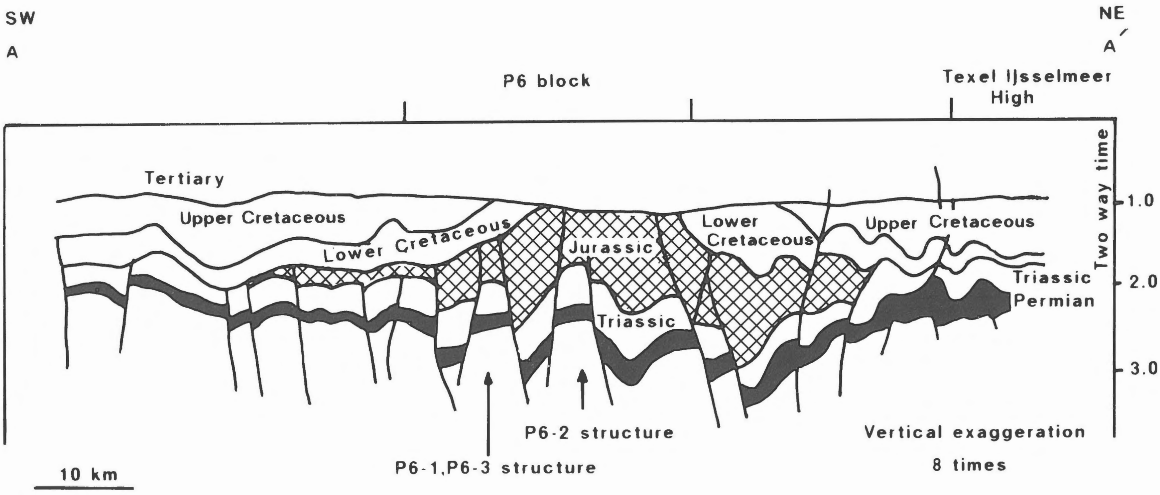

Fig. 2. Generalised geological cross section A-A°, showing the position of the P6-1, 3 and P6-2 structures.

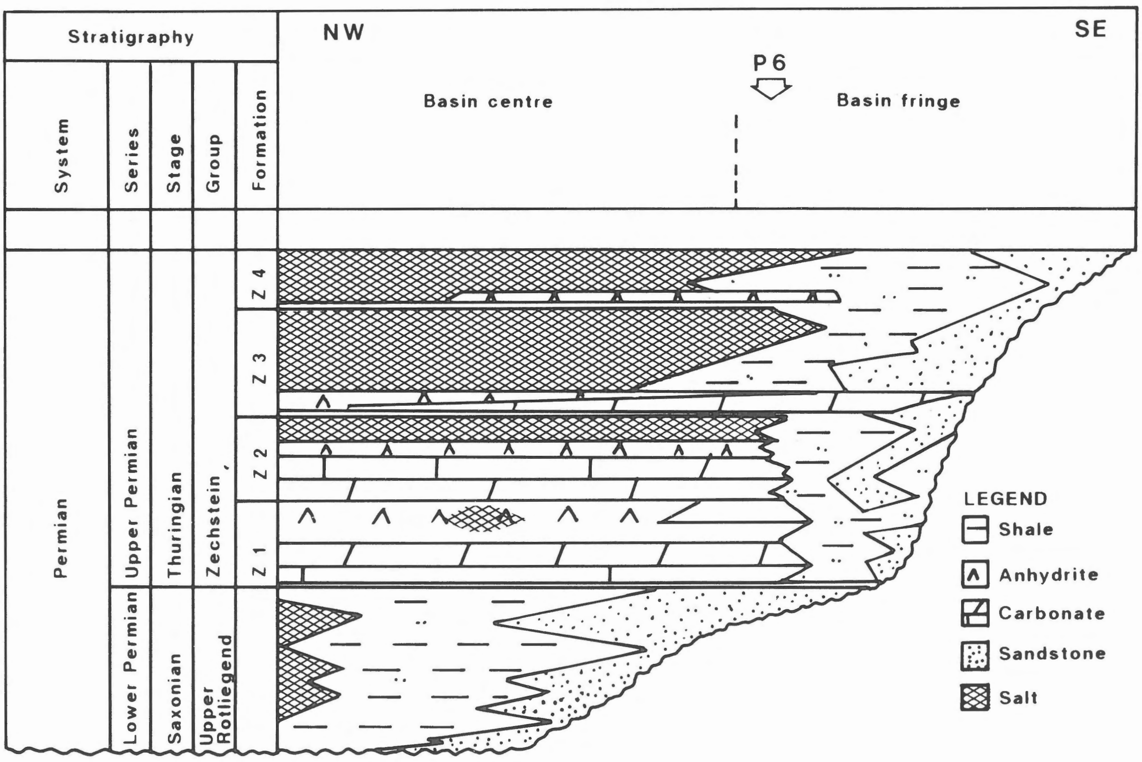

Fig. 3. Generalised stratigraphic column for the Permian in the Broad Fourteens area, modified after NAM & RGD (1980) and Van Adrichem Boogaert & Burgers, (1983). Note basin fringe position of P-6 Zechstein-3 Carbonates.

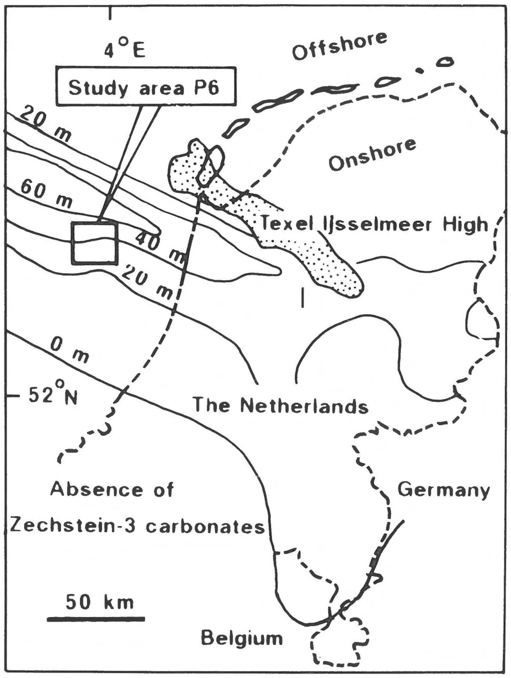

Fig. 4. Generalised isopach map of the Zechstein-3 carbonates (after Van Adrichem Boogaert & Burgers, 1983).

Methods

Cored Zechstein-3 carbonates were described and thin sections were petrographically investigated by means of conventional and cathodoluminescence microscopy. Some fifty thin sections were cut and partially stained with respectively Alizarin Red-s and potassium ferricyanide to allow distinction of calcite and ferroan calcite. The descriptions permitted interpretation of the sedimentary environment and reconstruction of the diagenetic sequence, including porosity development and destruction.

Subsidence curves were reconstructed for the studied area, taking into account Triassic sonic log velocities, stratigraphic thicknesses as encountered in wells and on seismic sections, maturation calculations by means of Lopatins method (Waples, 1980), LOM values (Hood et al., 1975) and vitrinite reflectivity measurements.

Porosity development and destruction are related to burial, taking into account environmental conditions during deposition of the sediments, the diagenetic sequences and the reconstructed subsidence curves.

Reservoir characteristics

In order to reconstruct porosity development, it is essential to establish the depositional characteristics of a sequence and relate diagenesis to the primary sediment characteristics. In addition timing, temperature and depth of burial of the different diagenetic phases need to be interpreted. In the following sections the depositional and diagenetic characteristics of Zechstein-3 carbonates are described.

Major lithologies and sedimentary units

An isopach map (Fig. 4) and a correlation section (Fig. 5) show the thickness of the Zechstein-3 carbonates in the P6 area. Study of the core material from wells P6-1, P6-2 and P6-3 led to a grouping of the sediments into four sedimentary units (Figs. 6 and 7), which are described below.

Unit 1: A salt-rich grey clay underlies Unit 1 with a gradational contact. Unit 1 consists mainly of dark grey to greyish black dolomites with argillaceous streaks. Minor anhydrite streaks and disseminated pyrite are present.

Unit 2: This Unit overlies Unit 1 with a gradual contact and consists of dark grey to greyish dolomites with argillaceous streaks. Some brecciated dolomites are present. Wavy bedding gives way to parallel bedding in the upper part of the sequence which consists of purer, tan coloured dolomites. This unit is gradationally overlain by Unit 3.

Unit 3: This Unit shows an upwards-decreasing dolomite content and an increasing shaliness. Nodular pyrite intervals are present. This Unit grades into Unit 4.

Unit 4: Shaly dolomites which in the upper part become increasingly reddish and silicious. Shales are platy and hard. Haematite, anhydrite, dolo-

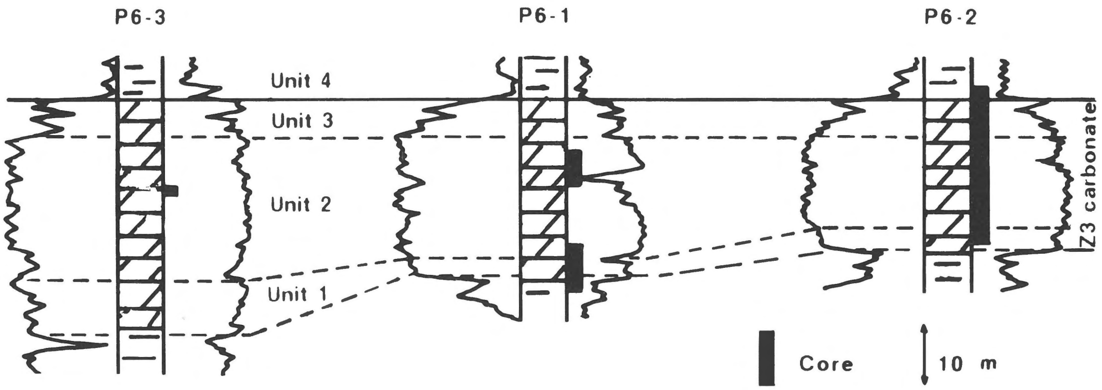

Fig. 5. Correlation section showing cored sections in wells P6-1, P6-2, P6-3. See Figs. 6 and 7 for details of cored intervals.

mite streaks and wavy bedding are locally present (Figs. 6 and 7).

Vugs and fractures, which may be lined with dolomite, and/or anhydrite are present in all intervals.

Sediment petrographical description

Aphanocrystalline to medium cyrstalline dolomites consisting of packstones/grainstones, packstones/wackestones, boundstones/packstones and breccias are present. Algae, shell fragments and peloids are mostly vague. Organic matter, anhydritised dolomite and pyrite are common. The partially stained thin sections showed that no ferroan calcite is present. In rare cases (see below) calcite is observed. The following facies types were recognised (Figs. 6 and 7).

Packstones/grainstones (Plate 1A). This microfacies consists of very fine to medium crystalline dolomite. Allochems consist of algae, forams, shell fragments and peloids and range in size from 100 μm to 2500 μm. Matrix crystal textures consist of xenotopic, hypidiotopic and idiotopic crystals. Fractures, filled with very coarse crystalline (replacement) anhydrite are present. Vuggy, intercrystalline, intraparticle, moldic and fracture porosity of up to 30% is observed.

Packstones and wackestones (Plate 1B). Very fine to medium crystalline dolomites. Allochems consist of algae, minor shell fragments and peloids, ranging in size from 100 μm to 2500 μm. The matrix consists of tightly packed, xenotopic, fine to medium crystalline dolomite. Shrinkage cracks, filled with very coarse crystalline anhydrite and also matrix replacing anhydrite are present. Intercrystalline, fracture and vug porosity is less than 5%.

Boundstones/packstones (Plate 1C). Aphanocrystalline to medium crystalline dolomite that is banded to laminated. Allochems, if present, comprise algae and peloids of up to 750 μm in size. The matrix is aphanocrystalline to medium crystalline xenotopic. Pore filling (Plate 1F) and replacement anhydrites, and also pyrite and shale partings are observed. Shrinkage cracks are filled with very coarse crystalline anhydrites (Plate 1C). Intercrystalline, fracture, vuggy and fenestral porosity is generally less than 5%.

Breccias (Plate 1D). Very fine to medium crystalline dolomite and calcite. Dolomite intraclasts range in size from 100–10.000 μm. Matrix dolomites and calcite comprise xenotopic and hypidiotopic textures. Stylolites, fractures and also minor organic material occur. Breccia and fracture porosity is less than 10%.

Log patterns

In well P6-2, four log patterns, corresponding to the informal sedimentary units 1 to 4 (Fig. 6) have

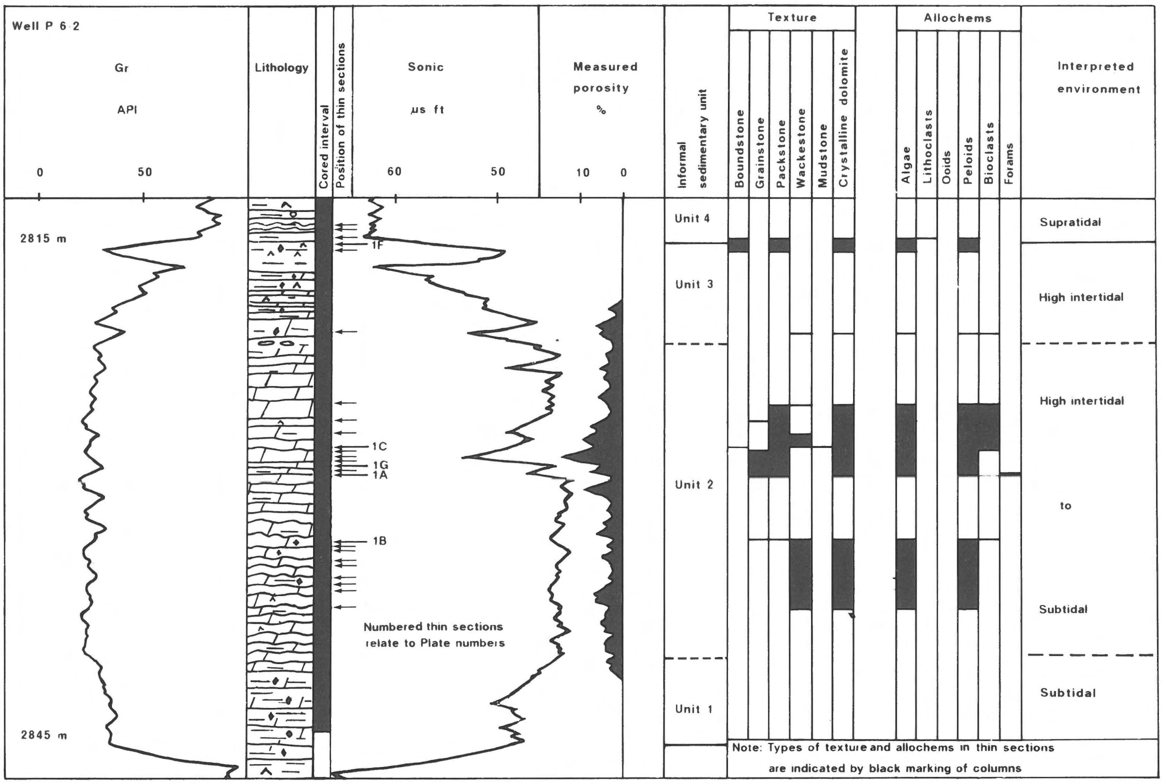

Fig. 6. Core description of well P6-2.

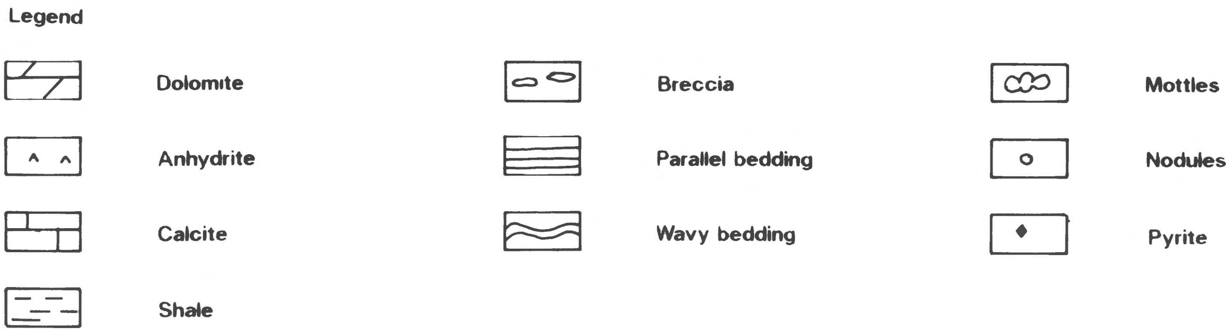

been identified on gamma ray and sonic logs. The correlation of these log patterns with wells P6-1, P6-3 is shown in Fig. 5 and demonstrates the continuity of the sedimentary units and the corresponding interpreted environments over the area.

Diagenesis and evolution of porosity

Diagenetic sequences (Figs. 8 and 9) were constructed from thin section observations (Plate I).

Early diagenesis includes lithification, and formation of shrinkage cracks in boundstones (Plate 1C), and also in wackestones (Plate 1B). A phase of early leaching affected mainly fossil fragments (Plate 1A). Intragranular, moldy (Plate 1A), vuggy porosity and fenestral porosity were formed during early diagenesis. Following dolomitisation, anhy-

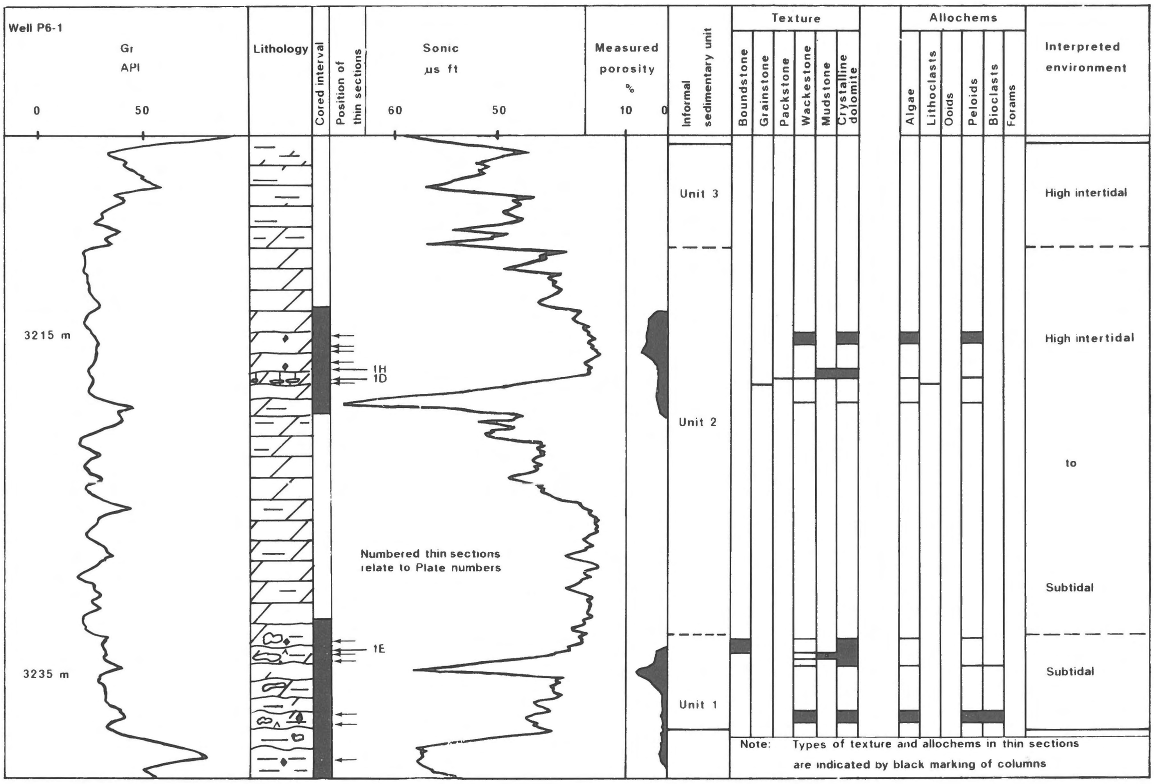

Fig. 7. Core description of well P6-1.

drite replacement (Plate 1E) and plugging of some pores (Plate 1F) took place. Calcitisation (Plate 1D) and also probably some late leaching (Plate 1G) was followed by compaction and stylolitisation (Plate 1B). Finally, fracturation increased porosity and permeability (Plate 1B and E).

Intragranular, moldy, vuggy (enlarged) intercrystalline- and fracture porosity occur in rocks investigated (Plate 1A, B, E, G and H). Early shrinkage cracks and fenestrae have all been plugged by anhydrite cements.

Hydrocarbon gas and CO_2 generation

It is generally accepted that the Upper Carboniferous Productive Measures are the principal source rocks for hydrocarbon gas in the basin (NAM & RGD, 1980; Oele et al., 1981). Most of the hydrocarbon gas is believed to have been generated at burial depths corresponding with vitrinite reflectances in the range 1.2 and 3.00 (Oele et al., 1981). Based on seismic sections, well data and lower Triassic shale velocity data, subsidence curves (Figs. 10 and 12) were constructed for the area, using the method described by Van Wijhe et al. (1980).

Maturation calculations were made for the P6-1, 3 structure. The vitrinite reflectances, calculated according to the method of Lopatin (after Waples, 1980) and Hood et al., (1975), are comparable to measured vitrinite reflectances of 0,8 at Zechstein level. Based on these data, most hydrocarbon gas, sourced in the Carboniferous sequence, is believed to have been generated during the Cretaceous (Fig. 10). It is likely that source rocks in the P6-1, 3 area, but not those in the P6-2 structure, reached their pre-inversion depths again during the Cainozoic and that renewed generation of hydrocarbon gas is continuing.

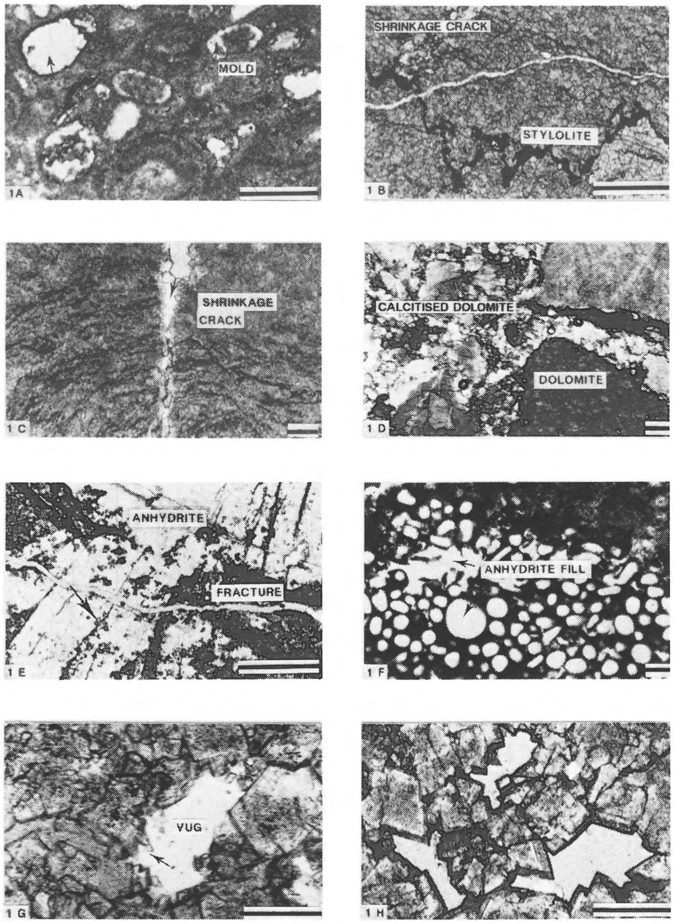

Plate 1. All photomicrographs taken with transmitted normal light.

A. Dolomitised packstone. Leaching of fossils formed moldy and vuggy porosity in a subtidal, intertidal environment. Location: P6-2. Depth: 2828,7 m. Scale bar 400 μm.

B. Dolomitised wackestone. An early shrinkage crack which was formed at the surface predates a stylolite which was formed at greater depths. A late fracture, probably formed during the Late Jurassic or Late Cretaceous, intersects and postdates the stylolite. Location: P6-2. Depth: 2833 m. Scale bar 400 μm.

C. Dolomitised boundstone. The shrinkage crack was formed early, after lithification, near the surface. After dolomitisation the crack was plugged by anhydrite during initial burial. Location: P6-2. Depth: 2827,5 m. Scale bar 400 μm.

D. Dolomitised breccia. Dolomite clasts are bedded in a dolomite/calcite matrix. Calcitisation was probably caused by CO_2 generation during burial. Location: P6-1. Depth: 3218 m. Scale bar 400 μm.

E. Anhydritised dolomite. Anhydritisation postdates dolomitisation as is evidenced by dolomite relicts (arrow). A fracture intersects and postdates anhydrite. Location: P6-1. Depth: 3243,3 m. Scale bar 400 μm.

F. Anhydritised packstone/boundstone. Anhydrite plugs intra- and vuggy porosity and postdates early leaching and dolomitisation. Location: P6-2. Depth: 2815,5 m. Scale bar 400 μm.

G. Crystalline dolomite. Corroded rhombs suggest late leaching during burial. Location: P6-2. Depth: 2828,6 m. Scale bar 400 μm.

H. Crystalline dolomite. Intercrystalline porosity, resulting from dolomitisation, is shown. Location: P6-1. Depth: 3217,9 m. Scale bar 400 μm.

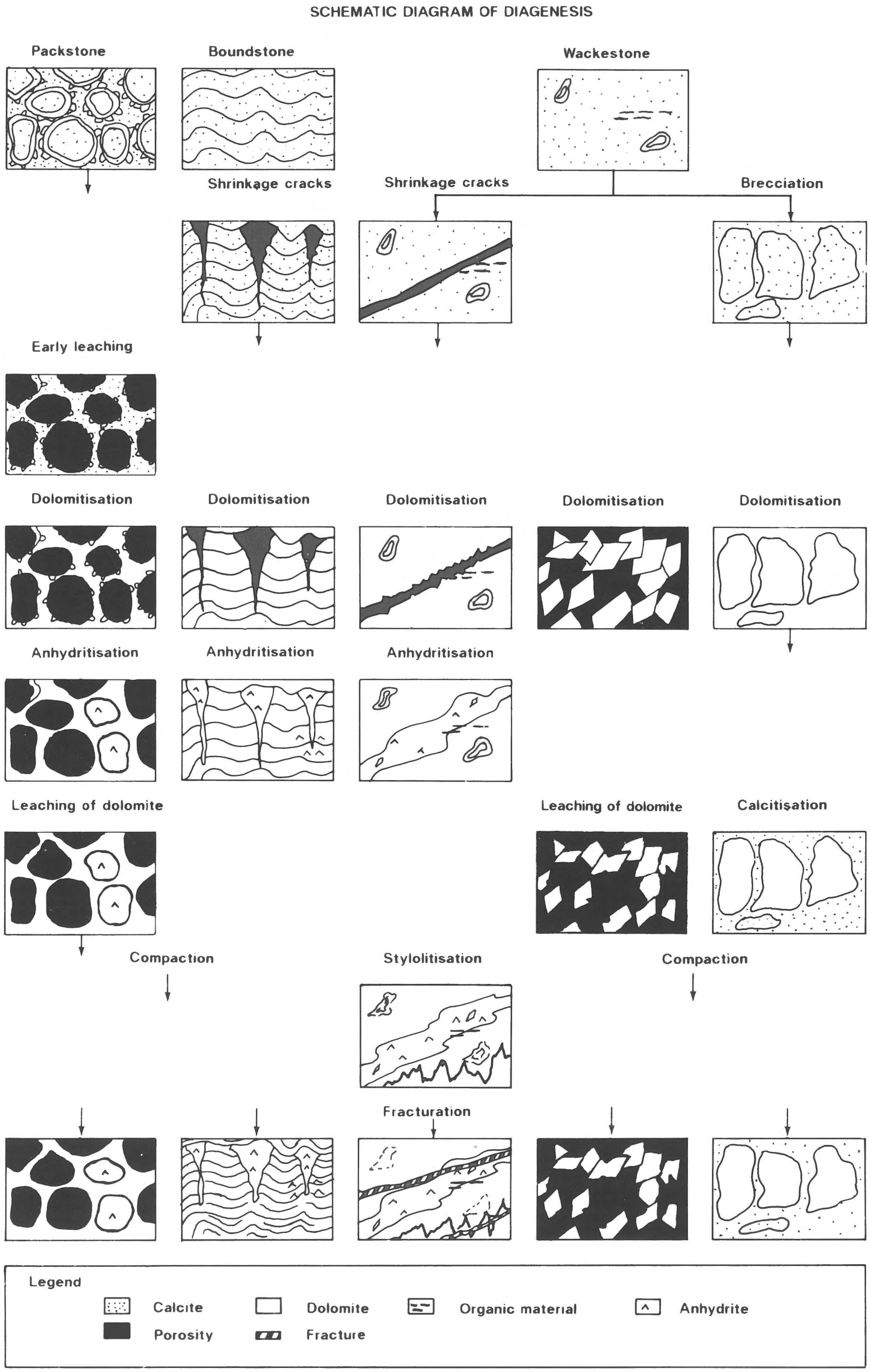

Fig. 8. Diagenetic features and interpreted diagenetic sequence. For explanation see text.

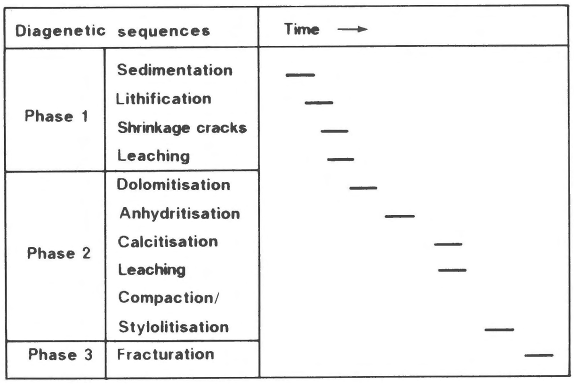

Fig. 9. Interpreted diagenetic sequence.

CO_2 gas is probably involved as a diagenetic agent. In general, CO_2 gas from humic source rock is generated at a stage with vitrinite reflectances ranging between 0,4–1,0 (Hunt, 1979). It is believed therefore (cf. Fig. 10), that some CO_2 gas was generated during burial.

Discussion

Following the deposition of Zechstein-2 evaporites, the sea transgressed and Zechstein-3 carbonates were deposited. They consist mainly of anhydritic boundstones, grainstones, packstones and wackestones. Fauna is sparse and the sequence is characterised by the presence of irregular fenestrae, algal structures, shrinkage cracks, breccia intervals and laminations. Towards the top the carbonates give way to increasingly shaly and non fossiliferous anhydritic dolomite deposits (Figs. 6 and 7). The presence of greyish, shaly dolomites with sparse fossils (algae and faunal bioclasts) and mottled structures points to a restricted, subtidal

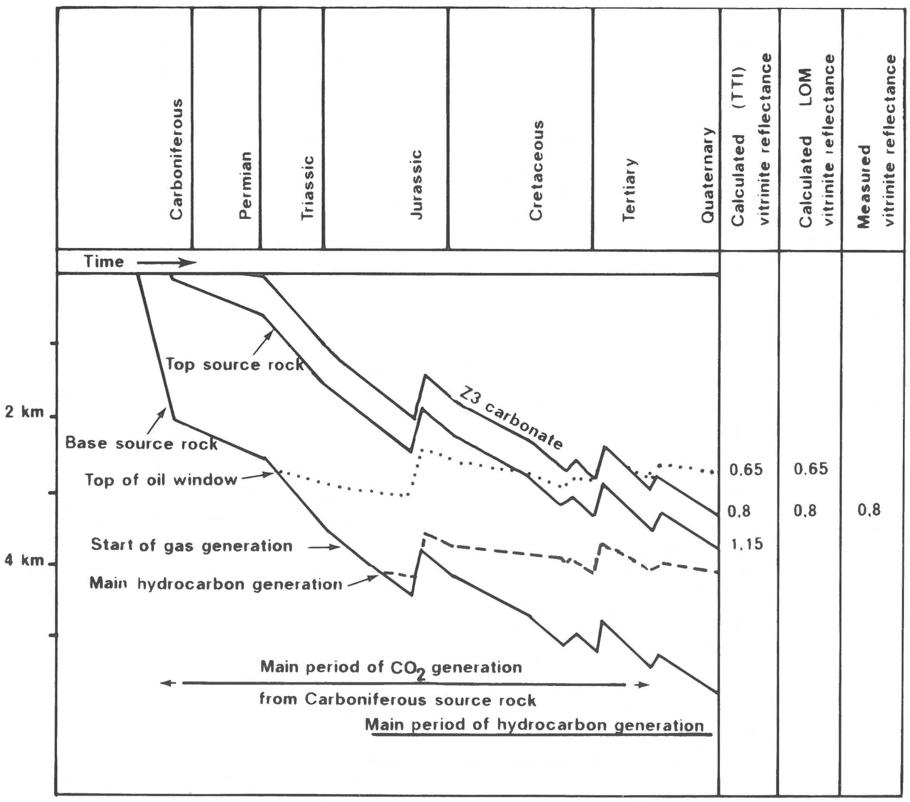

Fig. 10. Subsidence curve of Carboniferous source rocks in the P6-1, 3 area. Main hydrocarbon gas generation occurred during the Cretaceous and probably also during the Cainozoic. CO_2 gas was generated earlier than hydrocarbons.

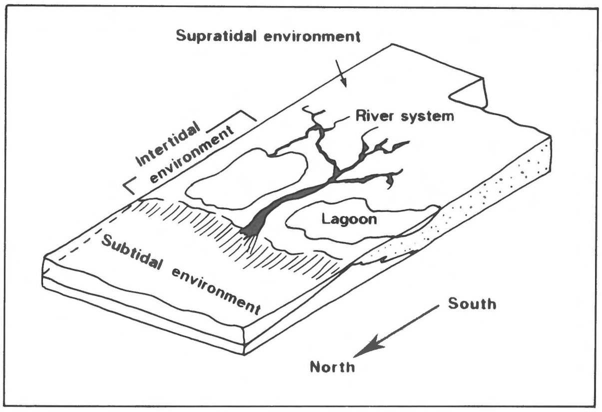

Fig. 11. Block diagram (after James, 1984) showing major morphological elements of a tidal flat. It is suggested that the Zechstein carbonates in block P6 were formed in a similar environment. In such a setting, leaching diagenesis is common.

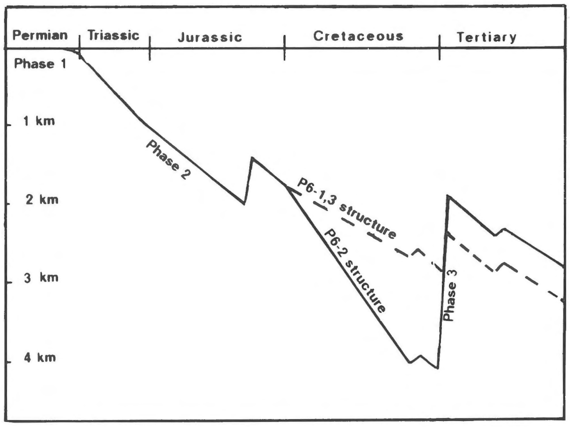

Fig. 12. Subsidence curves of the Zechstein-3 carbonates in wells P6-1, 3 and P6-2: P6-1, 3 structure is believed to be at maximum burial depth at present. Maximum burial in the P6-2 area was probably during the late Cretaceous.

setting for the base of the sequence (Unit 1) (cf. Shinn, 1983). The presence of sparse fauna and features such as irregular fenestrae, algal structures, shrinkage cracks, breccia intervals and laminations higher up in the sequence (Unit 2) indicates a high intertidal setting (cf. Shinn, 1983; James, 1984). The packstones/grainstones lithology with leached fossils points to a higher energy setting in such an intertidal environment. Towards the top of the sequence (Unit 3), a decrease of fossils, increasingly laminated, non-fossiliferous anhydritic dolomites and grey to reddish shales point towards shallowing-upwards from high intertidal carbonates to supratidal shales (cf. Shinn, 1983 and James, 1984). The total Zechstein-3 carbonate sequence corresponds to shallowing-upwards/regressive facies models as described by James (1984) and Shinn (1983). In such a setting (Fig. 11) diagenetic features for example leaching, dolomitisation and anhydritisation, as described for the Zechstein-3 carbonates, are quite common (cf. Shinn, 1983).

The diagenetic features (Figs. 8 and 9) are explained as follows: Following lithification, formation of shrinkage cracks and leaching of fossils may have taken place in an intertidal-supratidal environment, occurring during periods of low sea level. Dolomitisation and anhydritisation took place afterwards, during early burial, followed by calcitisation and also some leaching. This is explained as follows: Calculations on the maturation of source rocks and timing of gas generation (Fig. 10) have shown that CO_2-rich gas was generated during burial. Such gas, when moving upwards through carbonates may have contributed to calcitisation and also to some late leaching during burial (see also Clark, 1980b).

Continued burial caused compaction and stylolitisation. A late phase of anhydritisation, which was described by Stemmerik et al., (1987) for Danish examples, is not demonstrated with certainty in our material It is likely that the late fractures were formed at the time of Late Jurassic and/or Late Cretaceous tectonic activity.

The diagenetic phases were plotted on the burial graph (Fig. 12), taking above mentioned considerations into account. Of main interest to the oil and gas industry is that diagenetic porosity in carbonates has been available while renewed hydrocarbon gas generation continued.

Conclusions

Diagenetic porosity has been available while renewed hydrocarbon gas generation occurred. Interpreted diagenetic sequences indicate that early porosity was formed mainly during the Permian in a subtidal, intertidal to supratidal environment. Most of the early porosity was formed near the surface as a result of leaching and dolomitisation: leached intragranular, moldy, vuggy, (enlarged) intercrystalline porosity. Some minor, late leaching during burial is suggested. Late fracture porosity was formed in the subsurface probably during the Late Jurassic and/or Late Cretaceous.

Acknowledgements

I thank Prof. Dr. W. Viaene, Prof. Dr. R. Swennen (Catholic University of Leuven) and Dr. P. de Boer (State University of Utrecht) for comments on early versions of the manuscript. Also, comments and suggestions from a Geologie and Mijnbouw reviewer, have led to revisions, which improved the present paper. The Sedimentology Department at the State University of Utrecht kindly allowed the use of the cathodoluminescence apparatus. The Rijks Geologische Dienst of The Netherlands permitted investigation of core material.

References

Brueren, J.W.R. 1959 The stratigraphy of the Upper Permian 'Zechstein' formation in the eastern Netherlands. In: I Giacimenti Gassiferi dell Europa Occidentale – Atti del Conv. Milano 1957. I: 243–274.

Clark, D.N. 1980a The sedimentology of the Zechstein 2 carbonate formations of eastern Drenthe, The Netherlands. In: Füchtbauer H. & Peryt T. (eds): The Zechstein Basin with Emphasis on Carbonate Sequences – Contr. Sedimentol. 9: 131–165.

Clark, D.N. 1980b The diagenesis of Zechstein carbonate sediments. In: Füchtbauer H. & Peryt T. (eds): The Zechstein Basin with Emphasis on Carbonate Sequences – Contr. Sedimentol. 9: 167–203.

Clark, D.N. 1986 The distribution of porosity in Zechstein carbonates. In: Brooks, J., Goff, J.C., van Hoorn, B. (eds): Habitat of Paleozoic Gas in N.W. Europe Sc. Ac. Press. Ltd. Edinburg: 121–151.

Hood, A., Gutjahr, C.C.M. & Heacock, R.L. 1975 Organic metamorphism and the generation of Petroleum Am. Assoc. Petr. Geol. Bull. 59: 986–996.

Hunt, J.M. 1979 Petroleum geochemistry and geology – Freeman, W.H. & Co. (San Francisco: 617 pp.

James, N.P. 1984 Shallowing upward sequences in carbonates. In: Walker, R.G. (ed.): Facies models – Geoscience Canada, Repr. Ser. 213–228.

Oele, J.A., Hol, A.C.P.J. & Tiemens, J. 1981 Some Rotliegend gas fields of the K and L blocks, Netherlands Offshore (1968–1978)-a case history. In: Illing, L.V. & Hobson, G.D. (eds): Petroleum geology of the continental shelf of North-West Europe – Institute of Petroleum, (London): 289–300.

Maureau, G.T.F.R. & D.H. Van Wijhe 1979 The prediction of porosity in the Permian (Zechstein 2) carbonates of eastern Netherlands using seismic data – Geophysics 44: 1502–1517.

NAM & RGD (Nederlandse Aardolie Maatschappij B.V. & Rijks Geologische Dienst) 1980 Stratigraphic nomenclature of the Netherlands – Verh. Kon. Ned. Geol. Mijnbouwk. Gen. 32: 77 pp.

Shinn, E.A. 1983 Tidal flat environment. In: Scholle P.A., Bebout D.G., Moore C.H. (eds): Carbonate Depositional Environments. Am Assoc. Pet. Geol. Mem. 33: 171–210.

Stemmerik, L., Frykman, P., Winter Cristensen, O., Stentoft, N. 1987 The Zechstein carbonates of southern Jylland, Denmark. In: Brooks, J. & Glennie, K. (eds): Petroleum geology of North-West Europe. Graham & Trotman, London/Dordrecht/Boston: 365–374.

Van Adrichem Boogaert, H.A. & Burgers, W.F.J. 1983 The development of the Zechstein in The Netherlands – Geol. Mijnbouw, 62: 83–92.

Van der Poel, A.B. 1987 Porosity development in some uplifted carbonates of the Southern Permian Basin (Texel IJsselmeer High, The Netherlands, and The Hartz, Germany). In: Meded. Rijksgeol. Dienst, 's-Gravenhage, 41–1: 17 pp.

Van Lith, G.J. 1983 Gas fields of Bergen Concession. The Netherlands. In: Kaasschieter, J.P.H. & Reijers, T.J.A. (eds): Petroleum geology of the southeastern North Sea and the adjacent onshore areas – Geol. Mijnbouw 62: 63–74.

Van Wijhe, D.H., Lutz, M. & Kaasschieter, J.H.P. 1980 The Rotliegend and its gas accumulations – Geol. & Mijnbouw, 59: 3–24.

Van Wijhe, D.H., 1987 Structural evolution of inverted basins in the Dutch offshore – Tectonophysics: 137.

Visser, W.A. 1963 Upper Palaeozoic evaporites – Verh. Kon. Ned. Geol. Mijnbouwk. Gen., Geol. Ser. 21–2: 61–71.

Waples, D.W. 1980 Time and temperature in petroleum formation: application of Lopatin's method to petroleum exploration – Am. Assoc. Petrol. Geol. Bull. 64: 916–926.

Ziegler, P.A. 1982 Geological Atlas of Western and Central Europe – Elsevier: 130 pp.